Functional Nanoparticle-Augmented Surfactant Fluid for Enhanced Oil Recovery in Williston Basin

Quarterly Status Report
(for the period of August 1 through November 1, 2017)

Prepared for:

Karlene Fine
Brent Brannan

North Dakota Industrial Commission
State Capitol, 14th Floor
600 East Boulevard Avenue, Department 405
Bismarck, ND 58505-0840

Contract No.: G-041-081

Prepared by:
Hui Pu
Julia Zhao
Department of Petroleum Engineering
Department of Chemistry
University of North Dakota

Research Team Members:
Xun Zhong
Xiao Liu
Wen Sun
Xu Wu
Yanxia Zhou

October 25, 2017

Summary of Current Progress

During the past quarter, our primary goals are to start synthesizing and testing of different types of nanoparticles. Our focus is the characterization of nanoparticles and the stability test for those nanoparticles. We mainly focused on the following tasks:

1) Preparation and Characterization of PEG-coated Silica Nanoparticles for Oil Recovery;
2) Evaluation and Optimization of the nanoparticles and Nanoparticle-surfactant Hybrid for EOR;
   a.) Stability test of graphene oxide nanosheet (GON);
   b.) Stability test of partially reduced graphene oxide nanosheet (PrGON)
   c.) Stability test of Silica-Triton X-100 system
   d.) Stability test of Silica Nanoparticles

Below are the detailed results on the tasks.

1. Preparation and Characterization of PEG-coated Silica Nanoparticles for Oil Recovery

1.1 Introduction

Silica nanoparticles, produced via water-in-oil reverse micro-emulsion process, have been developed as a mature technique to produce size-controllable silica nanoparticles to apply in various fields. In recent years, sillia nanoparticles are reported to be used in oil recovery (He et al., 2015). To liberate the oil from rocks, the oil needs to be displaced from rock pores. The feasibility and efficacy of oil displacement mostly relied on interfacial interactions of solid–oil–water systems. Therefore, the physicochemical properties of oil, water and wettability of host solids are pivotal to this method. Surfactants can stabilize the emulsions and literate the oil from rocks. In order to enhance the oil recovery, surfactant has been tested to link onto the nanoparticle to enhance the efficacy of oil recovery. Suitably surface-coated nanoparticles will adsorb preferentially at oil/water interfaces, the recovery efficiency is enhanced.

Particle size of less than 100 nm is much smaller than rock pore channels so the nanoparticles can penetrate through the reservoir (Li et al., 2013). The fluid suspension of nanoparticles will extract the oil out of the rocks. In this report, PEG has been linked onto the surface of silica nanoparticles, various lengths of PEG have been linked onto the silica and corresponding characterizations have been showed. It has been reported that during the hydrolysis, the PEG surfactant will settle on the surface of silica nanoparticles (Andreani, 2014).

1.2 Experimental Section

Materials. Cyclohexane, 1-hexanol, ammonia water, triton X-100, ethanol and tetraethyl orthosilicate have been purchased from sigmal Aldrich. Polyethylene glycol with molecular weight of 400, 6,000 and 8,000 have also purchased from sigmal Aldrich.

Instrumentations. An Eppendorf 5804 centrifuge and ultrasonicator were used to wash, disperse, break and separate nanoparticles. A Zetasizer particle analyzer (Marlwen, model of Nano-ZS) was used to measure hydrodynamic diameters and surface charges of the nanomaterials. A Hitachi 7500 Transmission Electron Microscope (TEM) was utilized to

characterize the size and morphology of silica nanoparticles and PEG-coated silica nanoparticles (Xu, 2003).

Preparation of partially reduced graphene oxide nanosheet. Briefly, the PrGON was generated from graphene oxide. 40 mL, 2 mg/mL graphene oxide solution in water was added with 80 μL hydrazine hydride at 85 ℃, and stirred overnight. Then, the formed PrGON was purified by centrifugation at 10,000 rpm for 30 min and finally dispersed in water for further usage.

Synthesis of silica nanoparticle and PEG-coated silica nanoparticle. For the silica nanoparticles synthesis: 7.5 mL cyclohexane, 1.6 mL 1-hexanol and 1.8 mL Triton X-100 have been mixed together for 20 min. 480 μL distilled water was added and kept stirring for 20 min, followed by the addition of 100 μL ammonia water solution. Finally, 100 μL TEOS was added and stirred overnight.

For the PEG-coated silica nanoparticles: 7.5 mL cyclohexane, 1.6 mL 1-hexanol and Triton X-100 were added together for 20 min. Then, 480 μL distilled water was introduced into the system. After 10 min, 100 μL ammonia water solution and 100 μL of 8% PEG 400, 6000, or 8000 was added and stirred for 30 min. Finally, 100 μL TEOS was added and stirred overnight.

1.3 Results and discussion

Characterization of silica nanoparticles. After the preparation of the pure silica nanoparticles, we characterized the size, morphology, and zeta-potential of the silica nanoparticle. As shown in Figure 1, the pure silica nanoparticle without PEG modification shown mono-dispersed distribution in the SEM images. The images also showed that the morphology of silica nanoparticle is sphere. The size of the silica nanoparticles was calculated to be about 50 nm, which is smaller than that from the DLS measurements using zeta-sizer.

We also investigated the physiochemical properties of the PEG-silica nanoparticles. As shown in Figures 2-4, compared with the pure silica nanoparticle, PEG-silica nanoparticles formed significant aggregates in the SEM images. With the increase of the molecular weight of PEG from 400 to 6,000 and 8,000, the aggregation was more serious. Meanwhile, the diameter of the PEG-silica nanoparticles was also increased to about 75 nm in the PEG8000-silica nanoparticles, which is consistent with the trends in the DLS results (Table 1). However, from the measurements of the zeta-potential of the nanoparticles, the PEG modification of the silica nanoparticles induced a new peak at about -22 mV from the original -45 mV of the pure silica nanoparticles, indicating the successful modification of PEG on the surface.

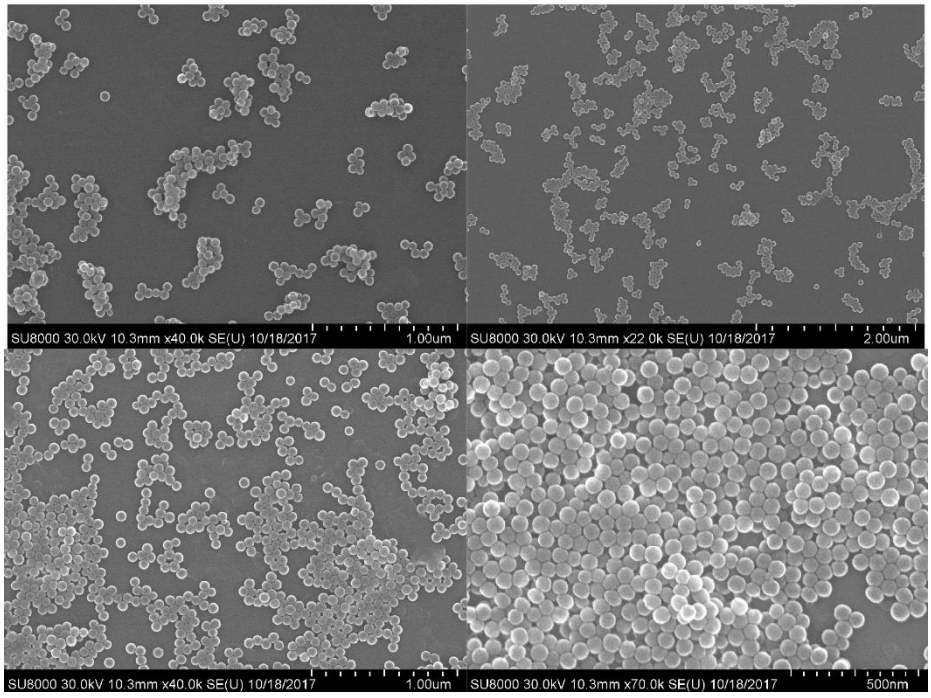

Figure 1. SEM images of the pure silica nanoparticles

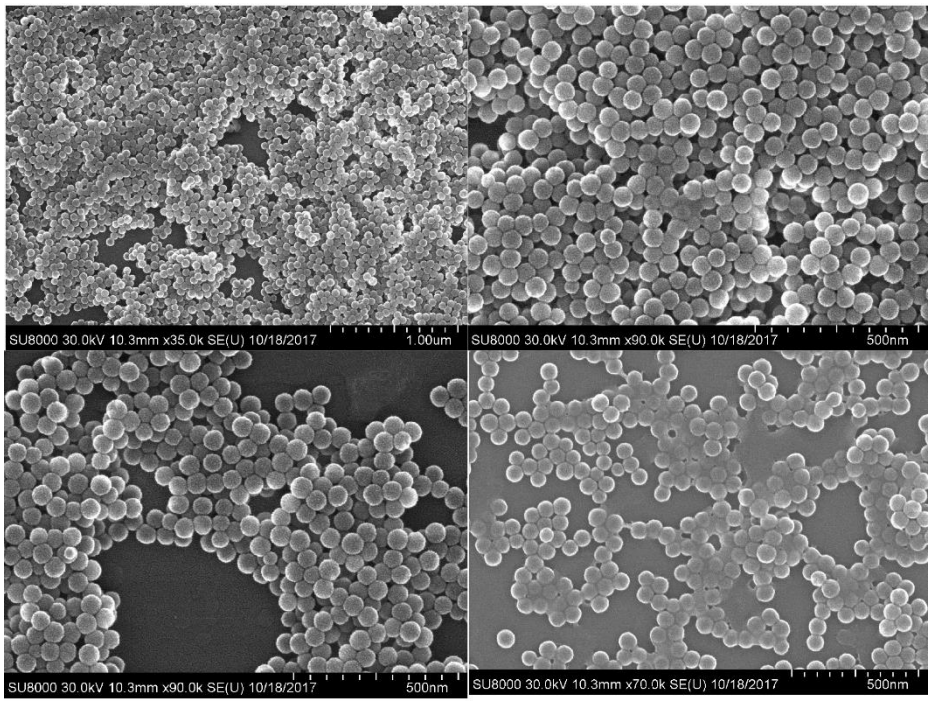

Figure 2. SEM image for PEG-400 silica nanoparticles

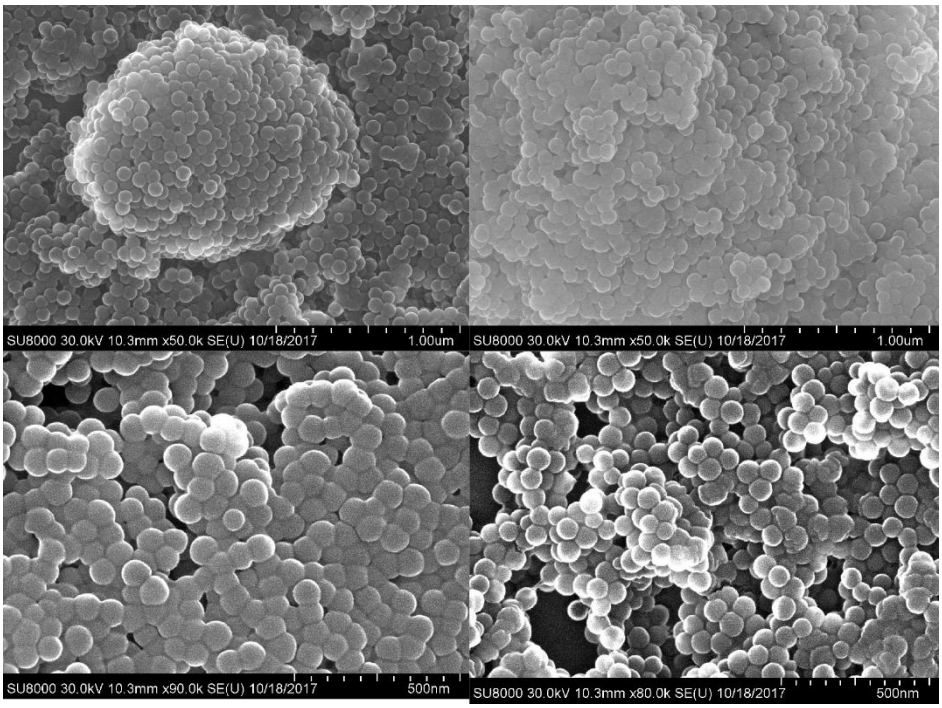

Figure 3. SEM image for PEG-6000 silica nanoparticles

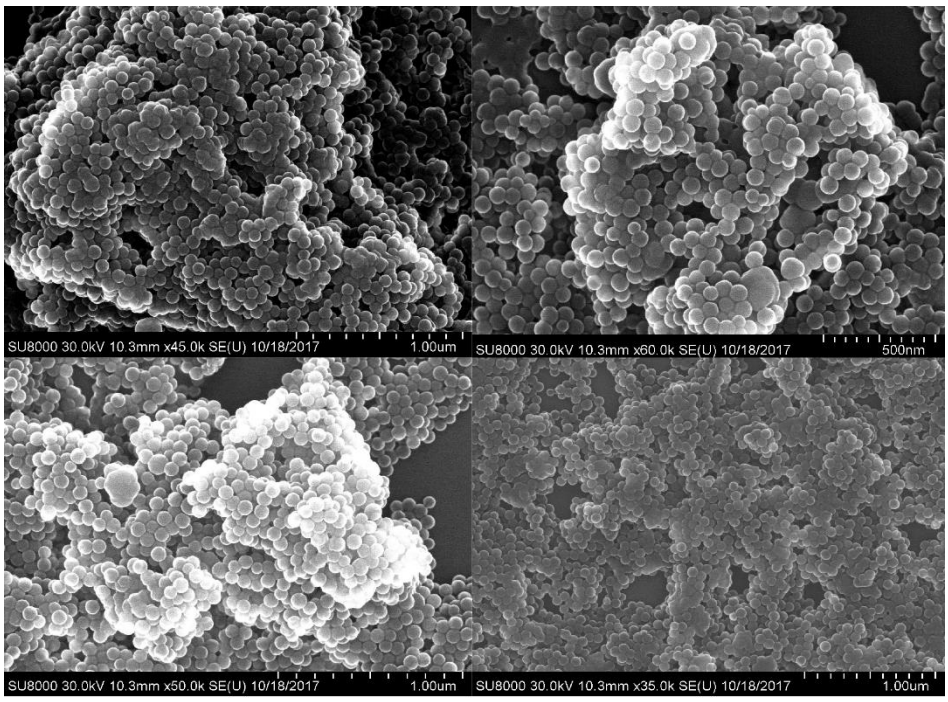

Figure 4. SEM image for PEG-8000 silica nanoparticles

Table 1. DLS measurements about the diameter and zeta-potential of the silica nanoparticles.

	Size(nm) DLS	Zeta Potential(mv)
Silica nanoparticles-PEG 8000	155-225 nm	-46mV, -22 mV
Silica nanoparticles-PEG 6000	133nm-190 nm	-47 mV, -20 mV
Silica nanoparticles-PEG 400	90-152 nm	-46 mV, -27 mV
Silica nanoparticles	70-110 nm	-45 mV

2. Evaluation and Optimization of the Nanoparticle-surfactant Hybrid for EOR

2.1 Introduction

Since nanoparticles dispersions are often unstable at high temperature, high pressure, and high salinity environments, particle agglomeration may easily happen, which not only renders the fluid ineffective but also causes severe damage to the formation. While effectiveness of surfactant solution to reduce oil-water interfacial tension (IFT) is impaired by the adsorption of surfactant in porous media and renders the process unfeasible (Curbelo et al., 2007). Large amounts of surfactants are required to produce small amount of extra oil if the adsorption is too high.

To increase the efficiency of both surfactants and nanoparticles, nanoparticle-surfactant augment system was introduced. Due to the large surface area of nanoparticles, they can be used as a promising surfactant carrier, which could compete with clay minerals and formation sand and thus reduce the unnecessary loss of expensive surfactants, and a lot more useful chemicals can move into the deep formation. Following are some applications and results of nanoparticle-surfactant augment systems.

Mohammad et al. (2015) used hydrophilic/partially hydrophobic nano silica (0.2 wt%) together with sodium dodecyl sulfate (anionic surfactant, 0.2 wt%), and found that the interfacial tension between the mixture and oil started with a rapid decrease in low surfactant concentration and followed by an increase at higher concentrations. Surfactant adsorption on rock surface was generally reduced in the presence of nanoparticle and this reduction was much more considerable for hydrophobic particles in all surfactant concentrations. Suleimanov et al. (2011) reported the use of nonferrous metal nanoparticles (70-150 nm) together with sulfanole-alkyl aryl sodium sulfonate (anionic surfactant), and obtained an increase in the efficiency of the oil displacement by 35%, compared to that obtained using a surfactant solution alone in a homogeneous porous medium and 17% in a heterogeneous porous medium at a temperature of 25 °C. Karimi et al. (2012) applied zirconium oxide nanoparticles (24 nm) and ethoxylated nonylphenol (nonionic surfactant), and found that the formation wettability could change from strongly oil-wet to strongly water-wet in at least 2 days. Zhang et al. (2017) used Mn-Zn ferrite nanoparticles together with PEG6000, and reported that PEG6000 (nonionic surfactant) would not affect the structure of

nanoparticles (no apparent XRD peaks shift), but particles with smaller size can be obtained in the PEG6000-added samples due to steric hindrance effect and stabilization properties of the PEG. Nurudeen et al (2017) found that the presence of SiO_2 and Al_2O_3 nanoparticles in SDS solutions are effective in reducing the surfactant adsorption onto the kaolinite. Fan et al. (2015) reported that GONP transport was surfactant type dependent, and SDBS (with the same charge) was more effective to facilitate GONP transport than Triton X-100.

2.2 Materials and Methodology

Materials

Brines with different compositions and salinities were prepared and used in stability tests. Table 2 shows the composition of Bakken formation brine used in the study, this brine composition is from the published paper by Lu et al (2014). Other brines (Table 3) were also used in the study for a purpose of comparison of nanoparticles performances in synthetic Bakken brine and other brines.

Table 2. Bakken formation brine (Lu et al., 2014)

Ions	Concentration, mg/L
Na^+	101,263
K^+	6,525
Ca^{2+}	17,157
Mg^{2+}	1,223
Sr^{2+}	1,168
Ba^{2+}	30.4
Cl^-	196,874
SO_4^{2-}	409
HCO_3^- Alkalinity	300
TDS	324,949.4
pH	7.35
Ionic Strength	7.05

Table 3. Other brines used in the experiments

Brines	Concentrations, mg/L
50% diluted Bakken formation brine	162,474
NaCl solutions	30,000, 60,000, 120,000, 240,000, 320,000
$MgCl_2$ solution	30,000mg/L
Graphene oxide nanosheet (GON)	See below mentioned
Partially reduced graphene oxide nanosheet (PrGON)	
Silica nanoparticle	Spherical and monodispersed
One-wash Silica-Triton X-100	In the presence of free surfactant molecule, diameter=50nm, Zeta potential=-32mV
Three-wash Silica-Triton X-100	No free surfactant molecule, Zeta potential=-50mV
58N	Alcohol ethoxylated, Amphoteric, Nonionic surfactant

Five types of nanoparticles were tested in the stability tests: Graphene oxide nanosheet (GON), Partially reduced graphene oxide nanosheet (PrGON), Silica nanoparticle, One-wash Silica-Triton X-100, Three-wash Silica-Triton X-100.

Graphene oxide (GO) is an intermediate material made up of a carbon skeleton with main functional groups, such as carboxyl, expoxy and ether groups and hydroxy groups. Its structure was presented in Figure 5. These functional groups enable chemical reactions of GON to form covalent and non-covalent bonds with other compounds. The normally used way to produce GO is Hummer's method, via oxidization of graphite with strong oxidizing agents (a combination of $KMnO_4$, $KClO_4$, $NaNO_3$ and H_2SO_4).

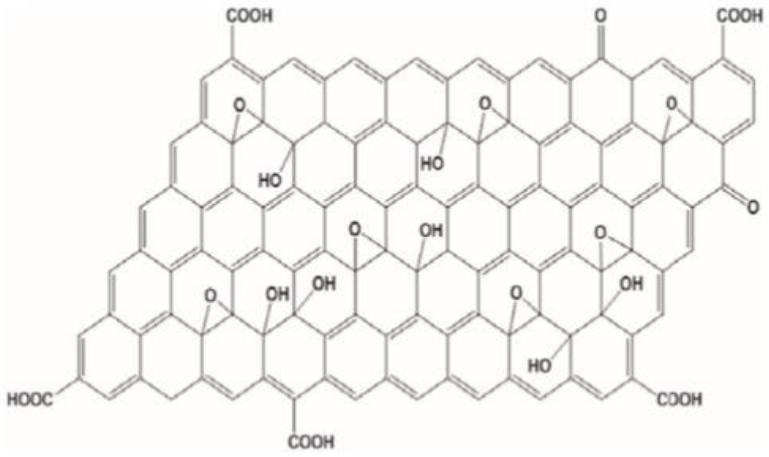

Figure 5. Graphene oxide structure

Generally, graphene oxides were obtained by oxidation of natural graphite powders with strong oxidants. The obtained GO were exfoliated into GON, and then were reduced to graphene by various reducing agents. After the reducing process, there will be less carboxyl on the graphene oxide nanosheet.

Silica nano particles are divided into P-type and S-type according to their structure. The P-type particles are characterized by numerous nanopores having a pore rate of 0.61 ml/g. The S-type particles have a comparatively smaller surface area. The P-type silica nano particles exhibit a higher ultraviolet reflectivity when compared to the S-type.

Triton X-100 ($C_{14}H_{22}O(C_2H_4O)_n$) is a nonionic surfactant that has a hydrophilic polyethylene oxide chain (on average it has 9.5 ethylene oxide units) and an aromatic hydrocarbon lipophilic or hydrophobic group. Undiluted Triton X-100 is a clear viscous fluid (but less viscous than undiluted glycerol) owing to the hydrogen bonding of its hydrophilic polyethylene oxide parts. Undiluted Triton X-100 has a viscosity of about 270 cp at 25 °C which comes down to about 80 cp at 50 °C. Triton X-100 is soluble at 25 °C in water, toluene, xylene, trichloroethylene, ethylene glycol, ethyl ether, ethyl alcohol, isopropyl alcohol, ethylene dichloride, but unless a coupling agent like oleic acid is used, Triton X-100 is insoluble in kerosene, mineral spirits, and naphtha.

2.3 Experimental methods

In this stage, emphasis was placed on stability test, including stability of surfactants, nanoparticles and nanoparticle-surfactant system. Static bottle testing is one of the simple and effective test methods used to test the stability of solutions and suspensions liquids. Although this kind of test is not representative of the real field conditions, it still can provide direct visual observation of surfactant turbidity and particle aggregation.

In this part, the effects of solutes concentration, solvent salinity and type, temperature were studied.

2.3.1 Selection of core samples

To thoroughly study the existence of surfactant and nanoparticle effect on imbibition is essential, also, the nanoparticles are expected to reduce surfactants' adsorption on formation rocks, so research on adsorption laws and affect factors are of great importance. In addition, core flooding experiment are essential to evaluate the effects and highlight the advantage of the researched optimal nanoparticle enriched surfactant fluid. Thus, different rock samples from different wells are needed to achieve the goals of this project.

For this research task, we tried to find out three wells in high production area, Well #15845, Well #17023 and #Well 19181. All the three wells are located in Mountrail County area. By choosing these three wells, we are eager to obtain an even permeability contrast (about 10) so as to better compare the imbibition rate and production rate in core flooding experiment, the core details are shown in Table 4.

Table 4. Core details

Well	Measured depth (ft)	Permeability (to air, mD)	Porosity (Ambient, %)
#15845	9641.00	0.0047	8.8
	9644.90	0.0058	8.1
#17023	9877.00	0.492	4.1
	9877.40	0.303	7.6
#19181	11221.5	0.032	5.5
	11226.5	0.039	5.8

2.4 Results and Discussions

2.4.1 Stability of graphene oxide nanosheet

To study the stability of graphene oxide, four sets of experiments were conducted, labeled as GO-1, GO-2, GO-3, and GO-4.

In GO-1, graphene oxide solutions were prepared using simulated formation brine at reservoir temperature (120 ℃) with concentration of 0.01 wt%, 0.02 wt% and 0.025 wt%. As shown in Figure 6, graphene oxide shown instability when first contacted with high salinity formation brine, so for the original state, the dispersions were not uniform. After being put into the oven at 120 ℃, sever particle aggregation could be observed in less than one day. Due to the large increase in particle size, nearly all the GON settled down at the bottom of the testing vials. The results were in accordance with the literatures, due to electrostatic cross-linking and destabilization of the negatively charged groups present on the GON sheets, particularly by the divalent calcium ions,

graphene oxide could not be stably dispersed at room temperature or above in brines which contained divalent ions.

(a) Initial (b) Day 1

Figure 6. Stability of GON in simulated formation brine

In GO-2, to create a less harsh environment, the concentration of divalent calcium ions in solvent was reduced by half through dilution. And the concentrations of graphene were decreased to 0.005 wt%, 0.001 wt% and 0.0005 wt%, testing temperature for this set was lowered to 105 ℃. As demonstrated in Figure 7, the stability of GON was not enhanced by environment change. From Figure 8, we can see that that GO particles have a very porous structure, especially after aging. It can be proposed that all functional groups exposed in brine environment, which may help to explain the property change of particles.

(a) Initial (b) Day 1

Figure 7. Stability of GO in 50% diluted synthetic formation brine

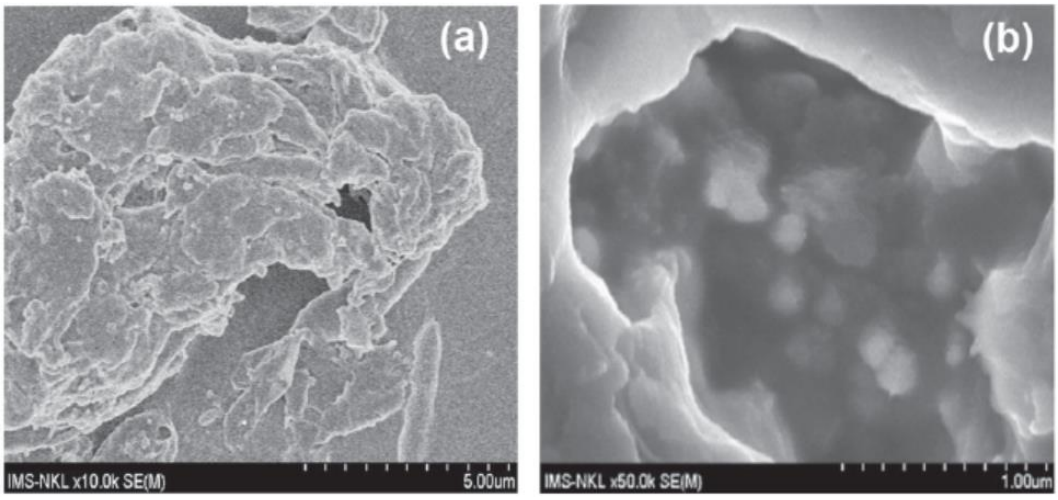

(a) Before aging (b) After aging

Figure 8. SEM pictures of GON in brine

GO-3 differed from GO-2 in solvent, with other conditions remained the same. In this set of experiment, distilled water was adopted. Figure 9 indicated that, particle aggregation was more obvious in relatively low particle concentration systems. There were two possible reasons for this phenomenon, one was that our eyes could not able to detect such a small morphology change, another one might be the increasing exposure area particles in lower concentrations.

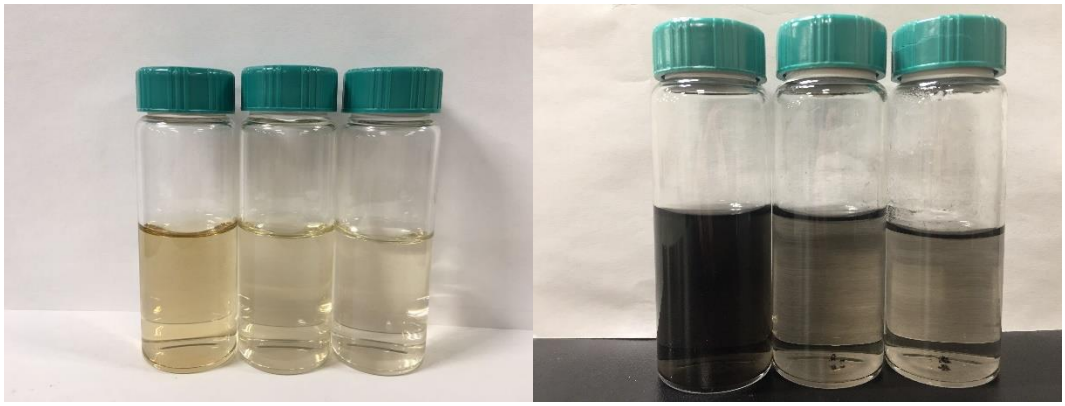

(a) Initial (b) Day 3

Figure 9. Stability of GON in distilled water

GO-4 was designed to study the effect of surfactant on the stability of nanoparticles in simulated formation brine at reservoir conditions (120 ℃), as presented in Figure 10. In this experiment, GON concentration was 0.02 wt%, and surfactant 58N was added directly to the GON dispersion. 58N is a nonionic surfactant which was reported to be stable at TDS more than 300,000mg/L, temperature 120 ℃ for as long as 14 days. Either due to GO properties change when first contacted with divalent ions or inadequate reaction between nanoparticles and surfactant, surfactant additive nearly had no effect on GO stability. In order to find out the exact explanation for this, more future researches need to be done, such as the effect of additive sequence, the reaction time and so on.

(a) Initial (b) Day 1

Figure 10. Stability of GON in simulated formation brine with surfactant

2.4.2 Stability of partially reduced graphene oxide nanosheet

The stability of PrGON was studied simply through two experiments conducted at simulated formation brine environment both at 120 ℃, one in the absence of surfactant (PrGON) concentrations were 0.01 wt%, 0.02 wt% and 0.025 wt%) and another in the presence of above mentioned surfactant 58N with PrGON concentration of 0.02 wt%, results were given in Figure 11 and Figure 12, respectively. After the reducing process, the carboxyl groups on GO particles reduced and the particle amount for the same weight concentration decreased significantly, since the cluster size was much smaller than that in GON stability test. However, neither GON nor PrGON was stable in reservoir conditions.

(a) Initial (b) Day 1

Figure 11. Stability of PrGON in simulated formation brine without surfactant

(a) Initial (b) Day 1

Figure 12. Stability of PrGON in simulated formation brine with surfactant

2.4.3 Stability of Silica-Triton X-100 system

One-wash silica-triton X-100 system (call OWST for short) is one type of nanoparticle-surfactant hybrid. Surfactants not only exist on nanoparticle surfaces but also present in the solution in free form. Solvent used to prepare dispersions was simulated Bakken formation brine. The test was separated into two parts according to OWST concentration, relative high concentration (0.005 wt% and 0.01 wt%, testing temperature=120℃) and lower concentration (0.005 wt%, 0.001 wt% and 0.0005 wt%, testing temperature=105℃) At first all the solutions were colorless and transparent. Both high concentration dispersions experienced a change in morphology in less than one day, as shown in Figure 13. While for the low concentration samples, there are some little dot sediments in the three bottles after 2 days, and 4 days later, the liquid surface in the first bottle (0.005 wt%) changed, as shown in Figure 14.

To better clarify the particle property change, particle size distribution curves were measured based on 0.005 wt% OWST and 0.001 wt% OWST, as shown in Figure 15. According to the data, both particles show great aggregation, which indicated that nanoparticle-surfactant systems used for Middle Bakken should be further modified.

(a) Initial (b) Day 1

Figure 13. Stability of OWST system (higher concentration) in simulated formation brine

(a) Initial (b) Day 2 (c)1st bottle, Day 2

Figure 14. Stability of OWST system (lower concentration) in simulated formation brine

(a) 0.005 wt% OWST (b) 0.001 wt% OWST

Figure 15. Particle size distribution curves for system

Three-wash Silica-Triton X-100 (call TWST for short) is another type of nanoparticle-surfactant hybrid system. In this system, surfactants only existed on nanoparticle surface. For this experiment, simulated formation brine was used to prepare 0.01 wt% and 0.02 wt% TWST solutions, testing at 120 ℃. Initially both solutions were colorless and transparent. After one day in high temperature, the solutions changed slightly, as shown in Figure 16, and we could see from the pictures that there were many white sediments in the two bottles. In the first bottle there are some dot sediments. In the second bottle there were some flocculent sediments. All these results indicated that TWST was unstable in high salinity water and high temperature environment.

(a) Initial state (b) Day 1

Figure 16. Stability of TWST system in simulated formation brine

2.4.4 Stability of Silica Nanoparticles

Silica nanoparticles were provided in two forms: nanoparticle solution, and dry solid particles. One is a silica nanoparticle solution with a concentration of 10mg/ml, another is dry powder.

Effects of salinity

In this part, experimental temperature and pressure were 80°C and 1atm, respectively. Dry solid silica nanoparticle was used to prepare 0.05 wt% nanoparticle dispersions. Seven solvents, distilled water, tap water, various NaCl solutions (30,000mg/L, 60,000mg/L, 120,000mg/L, 240,000mg/L and 300,000mg/L), as shown in Table 3. The aim for this experiment was to primarily test the stability of silica nanoparticle in different salinities of brines with monovalent ions.

Table 3 Seven solvents

	Distilled Water	Tap Water	NaCl Solutions				
Salinity (mg/L)	0	574	30,000	60,000	120,000	240,000	300,000

Initially all the seven nanoparticle solutions were cloudy. The sonification process was continued for 60 minutes to assure that nanoparticles had been homogenously dispersed. After 3 days, the solution changed apparently, as shown in Figure 17, from left to right the solvent is distilled water, tap water, 30,000mg/L, 60,000mg/L, 120,000mg/L, 240,000mg/L and 300,000mg/L. After 3 days, except the first bottle, there are many white sediments in the latter six bottles. Comparing with the first bottle (distilled water), there are many ions in the following six bottles. And because the nano solutions were made by dried solid nanoparticle, ultrasonic may not able to disperse the dried solid nanoparticle very well. Maybe this is also the main reason, so we will further test the salinity of simulated brine water to nano solution stability.

(a) Initial state (b) Day 3

Figure 17. The effects of salinity on the stability of silica nanoparticles (80℃)

Effects of temperature

Sample formulas used for this set of experiment were the same with the salinity part. Figure 18 showed that after 3 days, when the temperature is 20℃, the first and the second bottles did not change, while the rest 5 bottles have many white sediments. After 3 days, when the temperature is 80℃, the first bottle did not change, and the latter 6 bottles have many white sediments. From this, we can only draw a conclusion that silica nanoparticle is stable at both 20℃ and 80℃ when dispersed by distilled water. And stability at other temperatures will be tested later.

(a) Initial state (b) Day 3

Figure 18. The effects of salinity on the stability of silica nanoparticles (20℃)

Effects of nanoparticles concentration

Experimental temperature is 80°C, and solvent is 30,000mg/L NaCl solution. In this part, 10mg/mL silica nanoparticle solution was used to prepare 0.01 wt%, 0.02 wt%, 0.03 wt%, 0.04 wt% and 0.05 wt% silica nanoparticle solution (Solution I), and dried solid nanoparticle was used to prepare 0.1 wt%, 0.2 wt%, 0.3 wt%, 0.4 wt%, 0.5 wt% and 1.0 wt% silica nanoparticle solution (called Solid II).

Initially both the Solution I and Solution II were milk white. After 10 days, Solution I nearly have any changes, while Solution II changed significantly after 3 days, as shown in Figure 19. Ten days later, Solution I was still white milk and Solution II changed into transparent with many white sediments at the bottom, which indicated that when the concentration of silica nanoparticle is lower, the dispersions are stable at lower salinity. Also, we tested the particle size distribution of each solution, as shown in Figure 20. The size of silica nanoparticles was all around 100nm, which indicated that there was no agglomeration and silica nanoparticles were stable.

(a) Solution I: Initial

(b) Solution I: Day 10

(a) Solution II: Initial

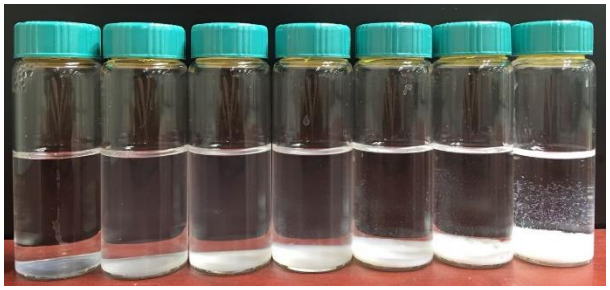

(b) Solution II: Day 3

Figure 19. The effects of concentration on the stability of silica nanoparticles (80℃)

Sample Name: Pdots-PVK-Eu-Temp 1
SOP Name: mansettings.nano
File Name: Silica-oil recovery2.dts
Record Number: 9
Material RI: 1.59
Material Absorbtion: 0.010
Dispersant Name: Water
Dispersant RI: 1.330
Viscosity (cP): 0.8872
Measurement Date and Time: Monday, October 16, 2017 4:11:29 ...
Temperature (°C): 25.0
Count Rate (kcps): 72.2
Cell Description: Disposable sizing cuvette
Duration Used (s): 100
Measurement Position (mm): 4.65
Attenuator: 11

		Size (d.nm):	% Number:	St Dev (d.nm):
Z-Average (d.nm): 1413	Peak 1:	179.5	100.0	23.62
PdI: 1.000	Peak 2:	0.000	0.0	0.000
Intercept: 0.867	Peak 3:	0.000	0.0	0.000

Result quality : Refer to quality report

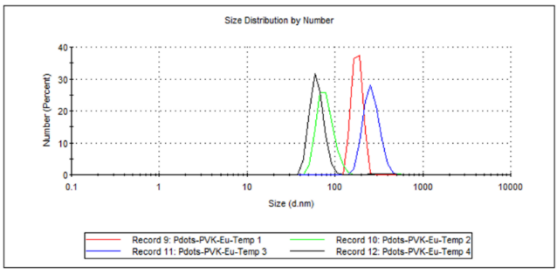

(a) 0.01 wt% SiNP

Sample Name: Pdots-PVK-Eu-Temp 3
SOP Name: mansettings.nano
File Name: Silica-oil recovery2.dts
Record Number: 15
Material RI: 1.59
Material Absorbtion: 0.010
Dispersant Name: Water
Dispersant RI: 1.330
Viscosity (cP): 0.8872
Measurement Date and Time: Monday, October 16, 2017 4:31:48 ...
Temperature (°C): 25.0
Count Rate (kcps): 372.5
Cell Description: Disposable sizing cuvette
Duration Used (s): 60
Measurement Position (mm): 1.05
Attenuator: 11

		Size (d.nm):	% Number:	St Dev (d.nm):
Z-Average (d.nm): 371.8	Peak 1:	1427	0.2	561.7
PdI: 1.000	Peak 2:	116.1	99.8	44.61
Intercept: 0.574	Peak 3:	0.000	0.0	0.000

Result quality : Refer to quality report

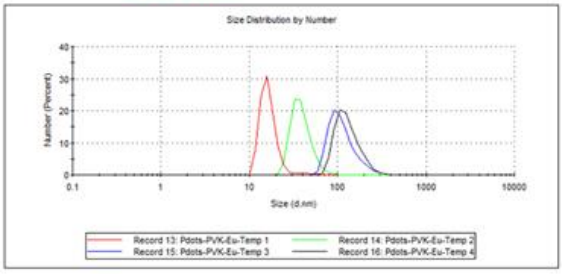

(b) 0.02 wt% SiNP

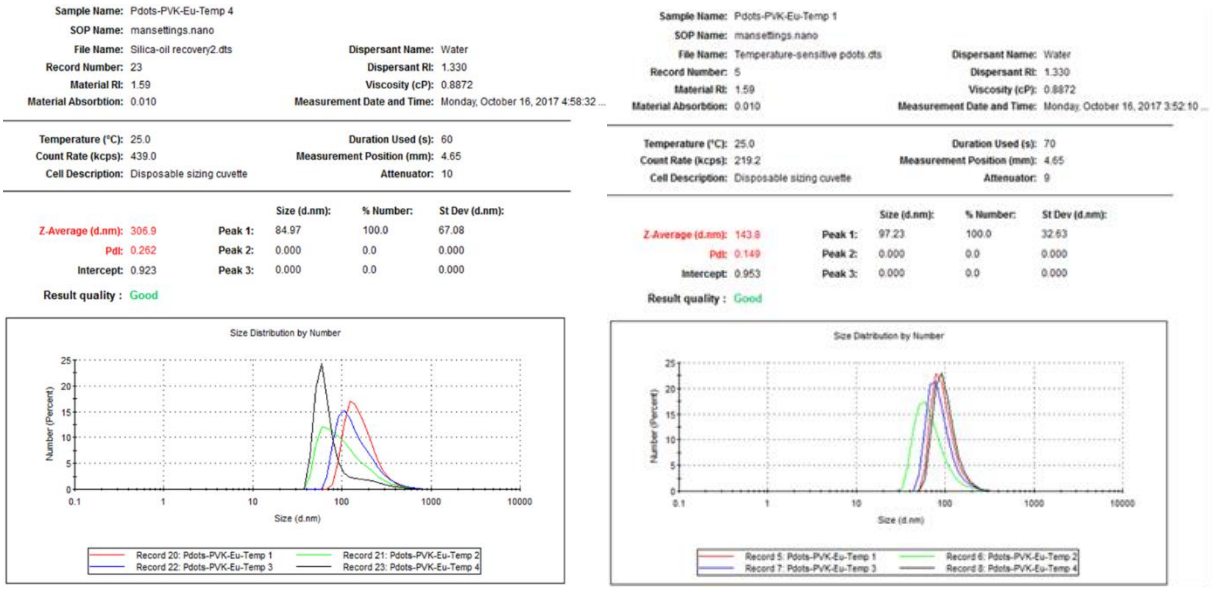

(c) 0.04 wt% SiNP (d) 0.05 wt% SiNP

Figure 20. Particle size distribution of various Silica nanoparticle dispersions

Effects of brine composition

In this part, three different solvents, 30,000mg/L NaCl solution, 30,000mg/L $MgCl_2$ solution and simulated Bakken formation brine were used to prepare 0.05 wt% silica nanoparticle dispersions at 80°C.

Initially all the solutions were milk white, as shown in Figure 21. After 3 days, all the three solutions changed into transparent with many white sediments at the bottom. This maybe also because of the unevenly disperse of dried solid nanoparticle powder. We will further test the nano solution stability by different composition of simulated brine water.

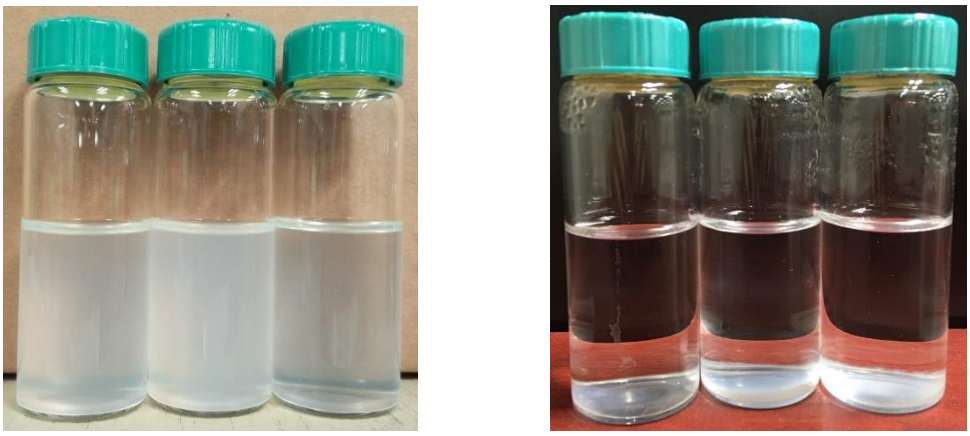

(a) Initial (b) Day 3

Figure 21. The effects of brine composition on the stability of silica nanoparticles (80℃)

Future Work

1. Prepare polymer nanoparticles, carbon nanoparticles, and porous silica nanoparticles as outlined in the proposal for investigation.
2. Reduce the size of the silica nanoparticles to less than 20 nm for fitting the requirement in the Bakken formation.
3. Modify silica nanoparticles with different types of surfactants to test the stability and oil recovery efficiency.
4.More stability test will be done based on nanoparticles, since the changes in type, size, wettability and electrical property will all have effects on the final results.
5. Measure the interfacial tension and conduct the adsorption test.

References

Andreani, T.; Souza, A. L. R. d.; Kiill, C. P.; Lorenzón, E. N.; Fangueiro, J. F.; Calpena, A. C.; Chaud, M. V.; Garcia, M. L.; Gremião, M. P. D.; Silva, A. M.; Souto, E. B., Preparation and characterization of PEG-coated silica nanoparticles for oral insulin delivery. International Journal of Pharmaceutics 2014, 473 (1), 627-635.

Aoudia M., Al-Maamari R. S., Nabipour M., Al-Bemani A. S.. Laboratory study of alkyl ether sulfonates for improved oil recovery in high-salinity carbonate reservoirs: A case study. Energy Fuels 2010, 24, 3655-3660.

Curbelo F. D. S., Sntanna V. C., Barros N. E. L., et al. Adsorption of nonionic surfactants in sandstones. Colloid Surf., A 2007, 293: 1-4.

Espinosa D. R., Caldelas F. M., Johnston K., et al. Nanoparticle stabilized supercritical CO2 foams for potential mobility control applications. In: SPE improved oil recovery symposium, Tulsa, OK; 2010.

Fan W., Jiang X. H., Lu Y.. Effects of surfactants on graphene oxide nanoparticles transport in saturated porous media. Science Direct, 2015, 35: 12-19.

He, L.; Lin, F.; Li, X.; Sui, H.; Xu, Z., Interfacial sciences in unconventional petroleum production: from fundamentals to applications. Chemical Society Reviews 2015, 44 (15), 5446-5494.

Hewakuruppu, Y. L., Dombrovsky, L. A., Chen, C., Timchenko, V., Jiang, X., Baek, S., Taylor, R. A.. Plasmonic pump–probe method to study semi-transparent nanofluids. Applied Optics. 2013, 52 (24): 6041–6050.

Ju B., Fan T.. Experimental study and mathematical model of nanoparticle transport in porous media. Powder Technol 2009, 192: 195-202.

Karimi A., Fakhroueian Z., Bahramian A., et al. Wettability alteration in carbonates using zirconium oxide nanofluids: EOR implications. Energy Fuels 2012, 26, 1028-1036.

Li, S.; Hendraningrat, L.; Torsaeter, O., Improved Oil Recovery by Hydrophilic Silica Nanoparticles Suspension: 2-Phase Flow Experimental Studies. International Petroleum Technology Conference, 2013.

Mohammad Z., Riyaz K., Nasim B.. Enhancement of surfactant flooding performance by the use of silica nanoparticles. Fuel, 2015, 143: 21-27.

Nurudeen Y., Muhammad A. M., Ahmad K. I.. Experimental investigation of minimization in surfactant adsorption and improvement in surfactant-foam stability in presence of silicon dioxide and aluminum oxide nanoparticles. Journal of Petroleum Science and Engineering, 2017, 159: 115-134.

Onyekonwu M. O., Ogolo N. A. Investigating the use of nanoparticles in enhancing oil recovery. Society for Petroleum Engineers (SPE) Conference Paper SPE-140744-MS, 2010, DOI: http://dx.doi.org/10.2118/ 140744-MS.

Schramm L. L. Surfactants: fundamentals and applications in the petroleum industry. United Kingdom; 2000.

Shahrabadi A., Bagherzadeh H., Roustaei A., Golghanddashti H.. Experimental investigation of HLP nanofluid potential to enhance oil recovery: A mechanistic approach. Society for Petroleum Engineers (SPE) Conference Paper SPE-156642-MS, 2012, DOI: http://dx.doi.org/ 10.2118/156642-MS.

Suleimanov B. A., Ismailov F. S., Veliyev E. F.. Nanofluid for enhanced oil recovery. Journal of Petroleum Science and Engineering 2011, 78: 431-437.

Wasan D. T., Nikolov A. D.. Spreading of nanofluids on solids. Nature 2003, 423, 156-159.

Wong K. V., Leon O. Applications of nanofluids: Current and future. Advanced Mechanical Engineering, 2010, 1-11.

Xu, H.; Yan, F.; Monson, E. E.; Kopelman, R., Room-temperature preparation and characterization of poly (ethylene glycol)-coated silica nanoparticles for biomedical applications. Journal of Biomedical Materials Research Part A 2003, 66A (4), 870-879.

Yu H., Kotsmar C., Yoon K. Y., et al. Transport and retention of aqueous dispersions of paramagnetic nanoparticles in reservoir rocks. In: SPE improved oil recovery symposium, Tulsa, OK, USA; 2010.

Zhang H. Q., Hua F., Zhang X. L.. Effect of PEG6000 on magnetic properties of the Mn-Zn ferrite nanoparticles. Journal of Magnetism and Magnetic Materials, 2017, 439: 245-250.